

Superfluid density reveals a quantum critical point between d-wave superconductivity and a Mott insulator

D. M. Broun,¹ P. J. Turner,¹ W. A. Huttmann,¹ S. Özcan,²
B. Morgan,² Ruixing Liang,³ W. N. Hardy,³ and D. A. Bonn³

¹Department of Physics, Simon Fraser University, Burnaby, BC, V5A 1S6, Canada

²Cambridge Laboratory, Madingley Road, Cambridge, CB3 0HE, United Kingdom

³Department of Physics and Astronomy, University of British Columbia, Vancouver, BC, V6T 1Z1, Canada
(dated: October 18, 2019)

In the phase diagram of the high T_c cuprates important clues for connecting the Mott insulator and the d-wave superconducting state can be found in the evolution of the superfluid density ρ_s with doping. ρ_s is the most fundamental property of a superconductor, measuring its ability to resist perturbations to the phase of the superfluid wavefunction. Here we report measurements of ρ_s in ultra-high purity $\text{YBa}_2\text{Cu}_3\text{O}_{6+x}$ as we continuously tune to the boundary of the superconducting phase, in a single sample, without changing cation disorder. We find that ρ_s becomes anomalously small, and has none of the features expected for the vortex unbinding transition of a 2-dimensional superconductor. The temperature dependence of ρ_s and a sublinear correlation between T_c and ρ_s , show that the approach to the insulating state is controlled by (3+1)-dimensional fluctuations of a strongly-paired superconductor in the vicinity of a quantum critical point.

Current research on high temperature superconductivity focuses on the underdoped cuprates, in a region of the phase diagram where d-wave superconductivity gives way to antiferromagnetism¹. It is here that the normal state of the cuprates is most at odds with Fermi liquid theory, with a pseudogap that persists above the superconducting transition temperature T_c and suppresses low energy spin and charge excitations^{2,3,4}. One proposal for this regime is that at temperatures up to about 100 K above T_c , superconductivity persists locally, with long-range phase coherence suppressed by fluctuations in the phase of the superconducting order parameter^{5,6,7,8,9}. Early results showing a linear relation between T_c and the superfluid density ρ_s ¹⁰ provided the original motivation for this point of view, suggesting that T_c is low in underdoped materials because the phase stiffness is low. Further support for this idea has come from measurements showing a finite phase stiffness above T_c at terahertz frequencies¹¹, and from experiments that appear to detect the phase-slip voltage of thermally diffusing vortices in the normal state¹². A set of alternative proposals based on gauge theories of the t(J) model predicts that the electron quasiparticles of the superconducting state evolve continuously into the spin excitations of an antiferromagnetic spin liquid, with the electrical current carried by the quasiparticles renormalizing to zero in the process^{13,14,15,16}. Testing these points of view now falls to experiment and measurements of the superfluid density are particularly well suited to the task. The superfluid density determines the phase stiffness | the resistance of the superconducting order parameter to fluctuations in its phase | and its temperature dependence provides a direct probe of the current carried by quasiparticle excitations. If the physics of the underdoped cuprates is indeed that of a fluctuating d-wave superconductor there should be a regime where quantum fluctuations come into play as T_c falls to zero with decreasing

doping. Scaling theory makes clear predictions for the form of the superfluid density near this quantum critical point^{17,18}. In this work we submit those predictions to a rigorous comparison with three different experiments. The tests rely on the high chemical homogeneity of crystals of $\text{YBa}_2\text{Cu}_3\text{O}_{6.333}$, and careful control of dopant homogeneity that gives sharp T_c 's even as $T_c \rightarrow 0$.

ρ_s is a tensor quantity that is usually determined by measuring the London penetration depth $\lambda_{\perp} / \rho_s^{1/2}$, which is the length scale over which supercurrents screen applied magnetic fields. Measurements of ρ_s face multiple challenges in underdoped $\text{YBa}_2\text{Cu}_3\text{O}_{6+x}$. Electronic anisotropy is greatly enhanced in these low doped samples¹⁹, with the ratio of c-axis to in-plane penetration depths $\lambda_c = \lambda_{ab}$ approaching 100. As a result, measurements of ρ_s can only be carried out in special geometries that drive purely ab-plane currents, such as the small single-crystal ellipsoid used in this work. The biggest challenge in approaching the quantum critical point is that T_c falls very rapidly with doping, requiring tight control of doping homogeneity^{20,21}. We have succeeded in producing samples with sharp superconducting transitions, and have also harnessed the process of CuO-chain ordering to fulfill a long-held ambition in strongly correlated electron materials | continuous tunability of the carrier density in a single sample, with no change in cation disorder¹⁹. In these high quality samples the loosely held dopant oxygen atoms in the CuO-chain layers remain mobile at room temperature. Once the average oxygen content is set and homogenized, gradual ordering at room temperature into CuO-chain structures slowly pulls electrons from the CuO_2 planes, smoothly increasing hole doping over time^{22,23}. The process is illustrated in Fig. 1. In the $\text{YBa}_2\text{Cu}_3\text{O}_{6+x}$ system a highly ordered phase should exist for $\text{O}_{6.333}$, the so-called Ortho- III^0 phase, in which every full chain is separated by two empty chains. At ambient pressure, the ordering

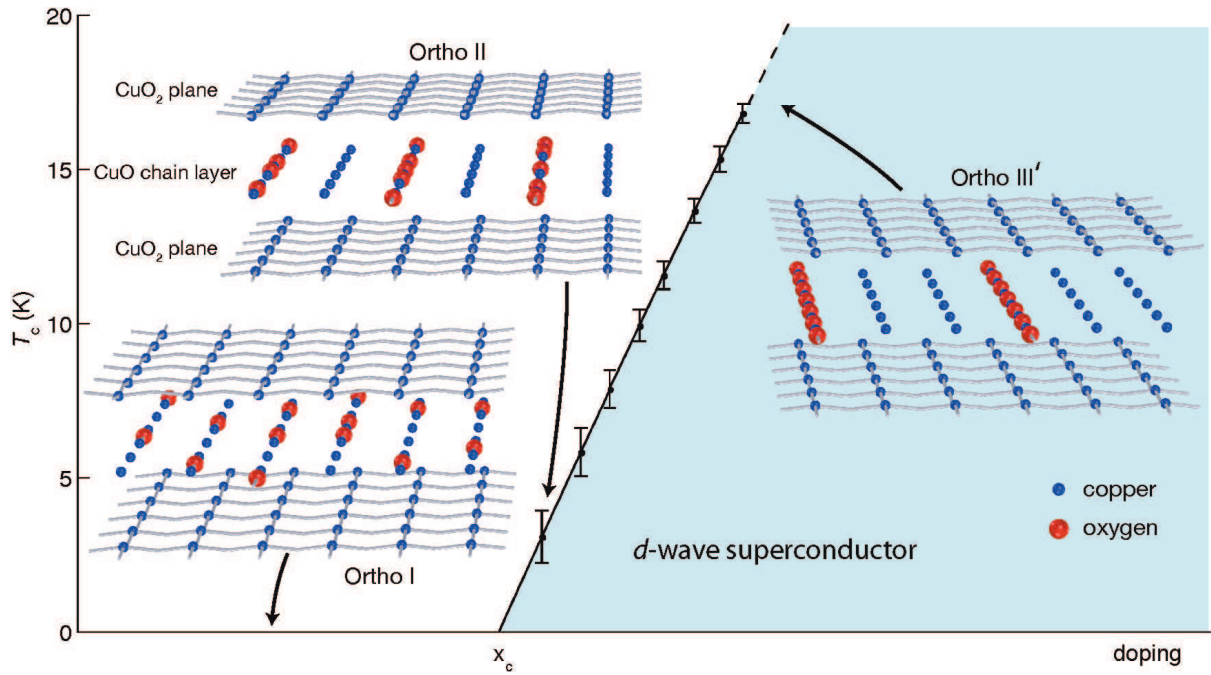


FIG. 1: Oxygen ordering in $\text{YBa}_2\text{Cu}_3\text{O}_{6.333}$ as a means of tuning doping. Crystal structures illustrate three states of CuO -chain ordering, each with the same oxygen content: defected Ortho I, formed after quenching from high temperature, in which oxygen sites in every CuO chain are randomly occupied; defected Ortho II, the stable room temperature phase at ambient pressure, in which every second CuO chain is empty; and the highly sought-after Ortho III' phase, in which full chains are separated by two empty chains. There is indirect evidence that the samples are approaching the Ortho III' phase by high pressure annealing: the transition width T_c , indicated by error bars, narrows markedly with increasing doping.

temperature of this phase is below room temperature, posing a barrier to its formation. High hydrostatic pressures should raise the ordering transition above room temperature, making it accessible. We have carried out extensive high pressure work in search of this phase and now have observed preliminary signs of the stabilization of Ortho III' order. The evidence is a marked narrowing of the superconducting transition width on the approach to the maximum T_c , as shown in Fig. 1. We are currently working to confirm these early indications with x-ray diffraction. The production of the Ortho III' phase is of vital importance, because it will enable a better gauge of the extent to which dopant randomness affects the fundamental physics of the cuprates. This degree of chemical homogeneity is not yet possible in other cuprate systems.

In our experiment the doping dependence of $\rho_s(T)$ has been obtained from a series of microwave surface impedance measurements, carried out at closely spaced doping intervals. All data sets were taken on one ellipsoidal single crystal, which was kept fixed in place for the duration of the experiment and tuned through the eight dopings using controlled room-temperature disordering of the chain oxygen, starting at $T_c = 17$ K. Figure 2a shows the surface impedance $Z_s = R_s + iX_s$ of the ellipsoid at two of the dopings, illustrating the normal-state matching of R_s and X_s used to obtain the absolute reactance. The transitions appear to be broad but this is

a consequence of fluctuations, not inhomogeneity of T_c . Figure 2b shows $\rho_1(T)$ at one of the dopings, with a sharp fluctuation peak at T_c . In the scaling theory of the superconducting transition²⁴, $\rho_1(T)$ is expected to have upward curvature throughout the fluctuation region, with a sharp cusp at T_c . In real samples there is rounding of the fluctuation peak, and we estimate the spread in T_c by equating T_c to the difference in inflection-point temperatures of $\rho_1(T)$ on opposite sides of the transition. The doping dependence of T_c is plotted in Fig. 1, where it is seen to sharpen in absolute terms with increasing oxygen order. Given the steepness of $T_c(x)$ in this doping range, the narrow transitions imply that the samples are highly homogeneous on macroscopic scales.

Strong scattering defects are present to some extent in all cuprate samples, and are known to drive a cross-over from linear to quadratic behaviour in $\rho_s(T)$ below a cross-over temperature $T^{25,26,27}$. The effects of pair breaking are expected to become more prominent as T_c gets smaller in the underdoped material. Nevertheless, our $\rho_s(T)$ data reveal a wide range of linear temperature dependence, as seen in Fig. 2c, with a sample-dependent T between 3 and 6 K, indicating an extrinsic origin of the low temperature curvature. The low temperature behaviour of $\rho_s(T)$, shown in Fig. 2d, is accurately quadratic, consistent with the strong-scattering theory. Oxygen disorder, an obvious candidate, is unlikely to be the source of pair-breaking, as T shows little change

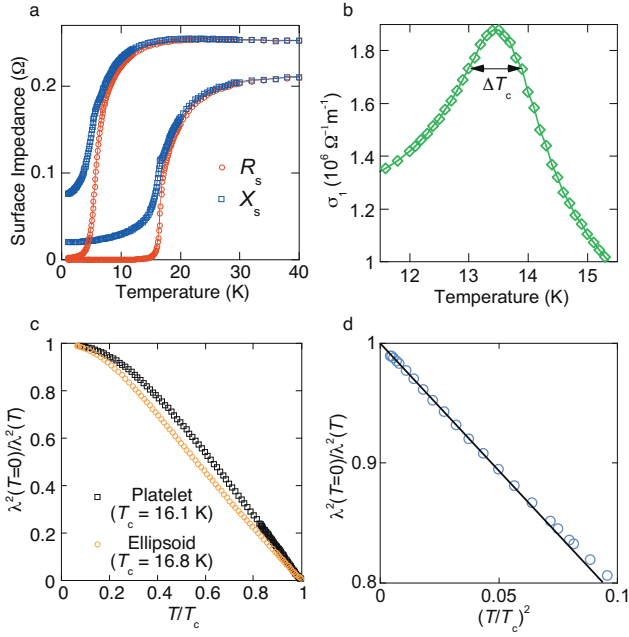


FIG. 2: Microwave spectroscopy and superfluid density. a, ab-plane surface impedance of the $\text{YBa}_2\text{Cu}_3\text{O}_{6+x}$ ellipsoid, at two dopings. $R_s(T)$ is measured directly in the experiment. Absolute reactance is obtained by offsetting $X_s(T)$ so that R_s and X_s match in the normal state. b, Real part of the conductivity $\sigma_1(T)$ obtained from the surface impedance, showing a sharp fluctuation peak at T_c . T_c is set to the difference between inflection points in $\sigma_1(T)$ on opposite sides of the transition. c, A comparison of $\sigma_1(T)$ for the ellipsoid and a much larger platelet crystal reveals sample-dependent curvature at low T . d, $\sigma_1(T)$ vs. T^2 , for the $T_c = 17$ K data set, shows that the asymptotic low temperature behaviour is quadratic, consistent with the effects of strong-scattering disorder.

with increasing ordering of the CuO chains.

Figure 3 shows $\sigma_s(T)$ at all eight dopings. The most striking feature of the data at the highest dopings is the wide range of linear temperature dependence, extending from T_c down to $T = 4$ K. Underdoped $\text{YBa}_2\text{Cu}_3\text{O}_{6+x}$ has a highly anisotropic electronic structure¹⁹, with $\frac{\sigma_c(T \rightarrow 0)}{\sigma_{ab}(T \rightarrow 0)} \sim 10^4$. The vanishingly small coupling in the c direction means that phase fluctuations in adjacent layers might be uncorrelated. As a result a Kosterlitz-Thouless (Berezinski) (KT) vortex unbinding transition^{28,29}, with an abrupt drop in σ_s , is expected when the 2D phase stiffness in a layer of thickness d , $\sigma_{2D}(T) \sim d^2 = 4k_B e^2 \rho^2(T)$, falls to $(2\pi)T$. This defines a minimum superfluid density, shown in Fig. 3 for both isolated CuO_2 planes and for coupled bilayers as the dashed and solid lines respectively. $\sigma_s(T)$ passes smoothly through this region, with no indication of a vortex unbinding transition or even of 3D critical fluctuations. Recent work has shown that the KT transition does occur in ultrathin $\text{YBa}_2\text{Cu}_3\text{O}_{6+x}$ films, but that the effective thickness for fluctuations is the

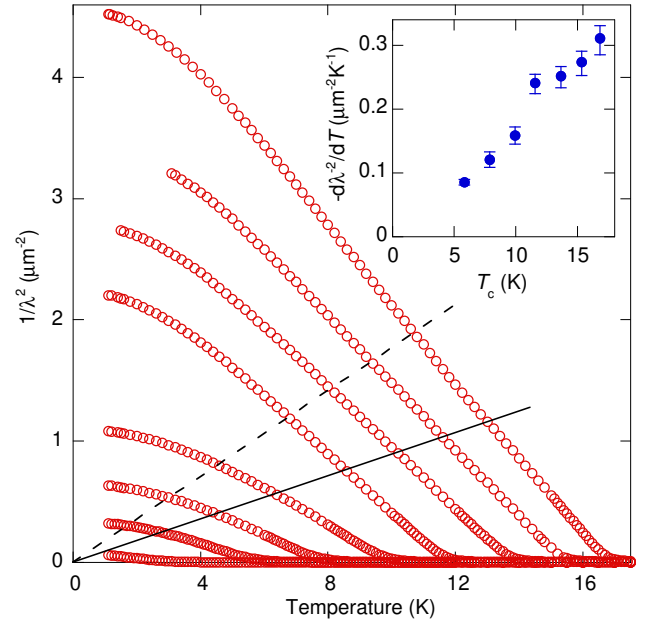


FIG. 3: Doping dependence of the superfluid density. $\sigma_s(T)$ of an $\text{YBa}_2\text{Cu}_3\text{O}_{6.333}$ ellipsoid, measured starting in the most ordered state ($T_c = 17$ K) followed by controlled oxygen disordering in small steps down to $T_c = 3$ K. Lines mark where the vortex-unbinding transition should occur for a 2-D superconductor. The dashed line corresponds to $\sigma_s = (2\pi)T$ in each CuO_2 plane, in units of temperature. The solid line shows $\sigma_s = (2\pi)T$ in each CuO_2 bilayer. The inset shows the temperature slope $|\partial \sigma_s(T)/\partial T|$ obtained from linear fits to $\sigma_s(T)$ between 4 K and T_c . Error bars represent the combined uncertainties in calibration, matching of R_s and X_s , and sample alignment.

film thickness³⁰. Our data support this and show that in bulk $\text{YBa}_2\text{Cu}_3\text{O}_{6+x}$ samples the transition is mean-field like. However, terahertz conductivity measurements on $\text{Bi}_2\text{Sr}_2\text{CaCu}_2\text{O}_{8+x}$ films show clear vortex unbinding at the expected minimum 2D superfluid density for bilayers³¹. Our data reveal a starkly contrasting situation in $\text{YBa}_2\text{Cu}_3\text{O}_{6+x}$. The linear depletion of $\sigma_s(T)$ all the way to T_c implies that spatial variations in the order parameter phase remain coherently locked together between adjacent layers, with the coherence extending over many unit cells in the c direction.

A central issue in the underdoped cuprates is whether the temperature dependence of the superfluid density is controlled by quasiparticle excitations or phase fluctuations^{28,29,31,32,33}. We have seen above that phase fluctuations, if present, are not acting in the way expected for a 2D superconductor. If instead quasiparticles played the dominant role, the low temperature superfluid response will be governed by excitations near the gap nodes. In that case

$$\sigma_s(T) = \sigma_0 \frac{2 \ln 2 k_B}{\sim^2 d} \frac{1}{v} \frac{v_F}{v} T; \quad (1)$$

where $\frac{v_F}{v}$ is the ratio of the quasiparticle group velocities

perpendicular and parallel to the Fermi surface and is the charge-current renormalization factor^{15,34}. In the inset of Fig. 3 we plot $\rho_{\parallel} = dT \rho_{\perp}$, which is proportional to $\frac{2v_F}{v}$. At low dopings the slope decreases approximately linearly with T_c . In this range v_F is known to vary only weakly with doping³⁵. The decrease in $\rho_{\parallel} = dT \rho_{\perp}$ is unlikely to be due to a divergence of v , instead indicating a strong variation of the charge current renormalization with doping. Such behaviour could be arising in several ways. Within the Fermi liquid framework, weak residual interactions between electrons can lead to backflow currents, reducing the total electrical current carried by a quasiparticle^{16,28,31,34}. Alternatively, in some distinctly non-Fermi-liquid theories of the under-doped cuprates, such as the slave-boson gauge theories of Anderson's resonating valence bond model^{3,14,15,16}, the superconducting quasiparticle is a combination of a chargeless spinon and a spinless holon, with an effective charge that shrinks to zero upon underdoping. U(1) and SU(2) gauge theories^{14,15,16} predict $\frac{2}{s_0}$, a result also obtained in theories of fluctuating d-wave superconductors^{7,8,9,32}. The observed doping dependence of ρ_{\parallel} , however, is much weaker than predicted.

An alternative cause of the decline in $\rho_{\parallel} = dT \rho_{\perp}$ could be the onset of microscopic phase separation with underdoping, resulting in a gradual rescaling of $\rho_{\parallel}(T)$ in proportion to the decreasing superconducting volume fraction. In less clean cuprates such as $\text{Bi}_2\text{Sr}_2\text{CaCu}_2\text{O}_{8+x}$ there is certainly evidence of nanoscale inhomogeneity in low-doped material³⁷. However, examination of the c-axis superfluid response indicates that such a scenario is unlikely in underdoped $\text{YBa}_2\text{Cu}_3\text{O}_{6+x}$. In Fig. 4 we plot the paramagnetic part of the superfluid density, $\rho_{\parallel}(T) - \rho_{\parallel}(T=0) = \rho_{\parallel}(T)$, which is sensitive to the energy spectrum of the nodal quasiparticles and directly probes their current response³⁸. For in-plane currents, $\rho_{\parallel}(T)$ fans out with doping, a consequence of the doping dependent slope. In contrast, for currents perpendicular to the CuO_2 planes, $\rho_{\parallel}(T)$ collapses onto a single, doping-independent curve away from T_c . The c-axis data are consistent with a negligible doping dependence of v_F and v , and strongly suggest that there is no change in the superconducting volume fraction with doping. The decline of $\rho_{\parallel} = dT \rho_{\perp}$ is seen to be purely a property of the in-plane quasiparticles, indicating that they are very different from the physical electrons that tunnel between layers.

The anomalous behaviour of $\rho_{\parallel}(T)$ revealed by our experiments has stimulated new theoretical work. Herbut has shown that the problem of nodal quasiparticles coupled to strong phase fluctuations maps onto the weakly interacting, anisotropic 3D Bose gas, due to the short-ranged nature of the Coulomb interaction in layered superconductors^{32,33}. In that model $\rho_{\parallel}(T)$ should be given at low dopings by the condensate fraction of a noninteracting Bose gas, $\rho_{\parallel}(T) = T \ln(T=t)$, with t the interlayer Josephson coupling. This correctly captures the linear T dependence of $\rho_{\parallel}(T)$ and the lack of a crit-

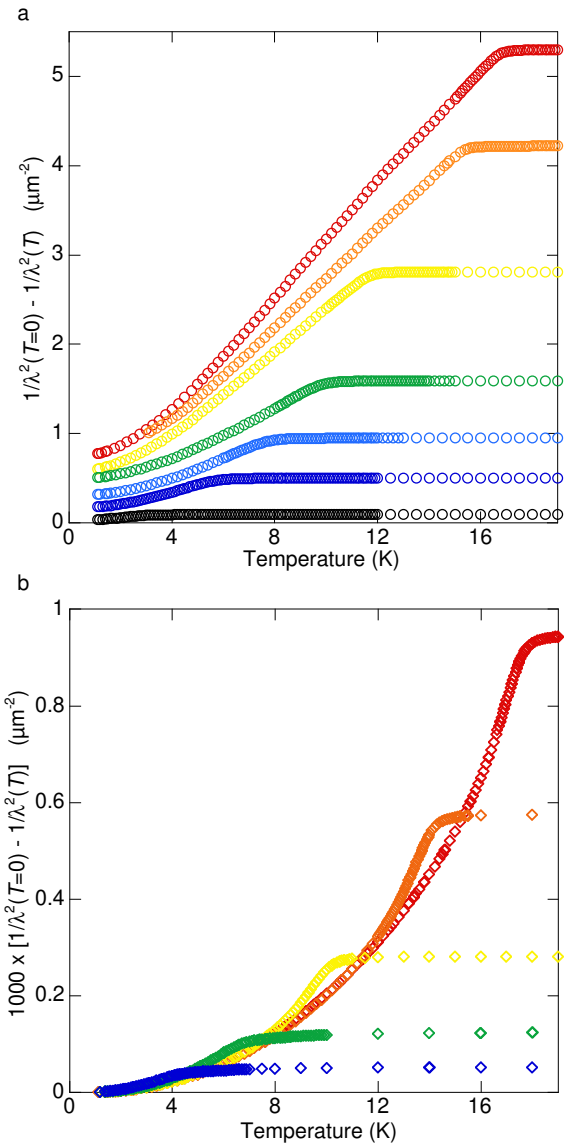


FIG. 4: Anisotropy of the normal fluid density. $\rho_{\parallel}(T) - \rho_{\parallel}(T=0) = \rho_{\parallel}(T)$ is a probe of the supercurrent carried by quasiparticle excitations close to the d-wave gap nodes, and is sensitive to the effects of charge-current renormalization. a, For currents within the CuO_2 planes, $\rho_{\parallel}(T)$ fans out with doping, revealing a clear increase in temperature slope. b, For currents perpendicular to the CuO_2 planes, all the $\rho_{\parallel}(T)$ data coalesce onto a common curve, independent of doping. This suggests that c-axis currents are not renormalized, and argues against microscopic phase separation as the cause of the unusual behaviour of the in-plane superfluid density. $\rho_{\perp}(T)$ data are taken from Ref. 19. For clarity not all data sets are shown.

ical region, but is at odds with the decline of $\rho_{\parallel} = dT \rho_{\perp}$ as $T_c \rightarrow 0$. Chen et al. have studied the BCS to Bose-Einstein condensate crossover as a model of strong correlation in cuprate superconductors⁴². In that theory, Cooper pairs can be thermally excited from the condensate without unbinding. The Cooper pairs contribute an

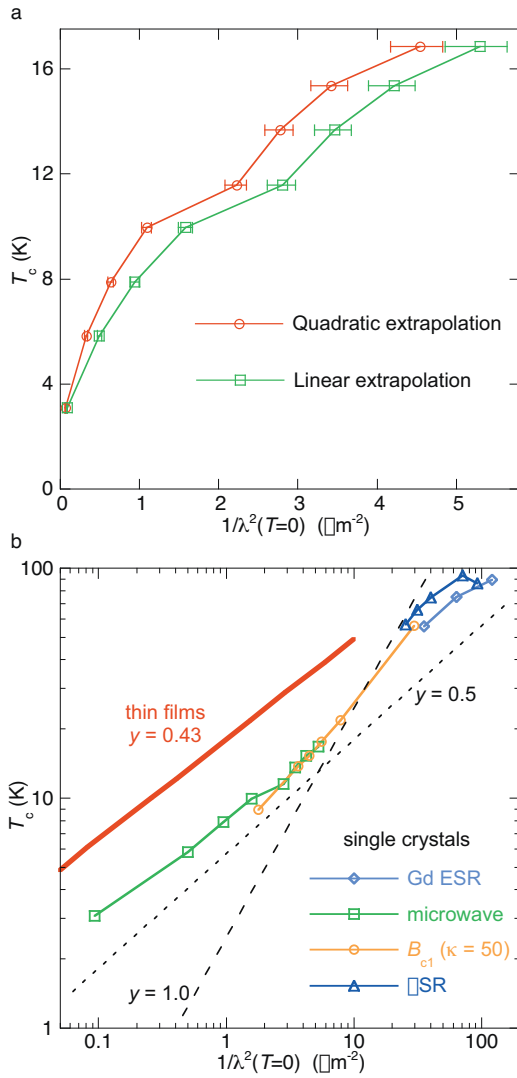


FIG. 5: Correlation between T_c and the zero-temperature superfluid density. $s_0 = 1/\lambda^2(T=0)$ is obtained by both linear and quadratic extrapolation to $T = 0$. a, T_c vs. s_0 on a linear scale, with error bars that indicate the combined uncertainties in calibration, κ setting of X_s , and sample alignment. b, T_c vs. s_0 , on logarithmic axes, over the full doping range of the $\text{YBa}_2\text{Cu}_3\text{O}_{6+x}$ system. Shown are data from: Gd^{3+} ESR, taking the geometric mean of a and b -axis values³⁹; lower critical field³⁶, assuming $\kappa = 50$; new μSR data on single crystals⁴⁰; and microwave cavity perturbation. Dashed lines indicate different power laws, $T_c \propto \lambda^{-y}$. T_c decreases smoothly over more than 3 decades of superfluid density, with a sublinear correlation extending over the whole range. For comparison we include data for $\text{YBa}_2\text{Cu}_3\text{O}_{6+x}$ thin films⁴¹, showing with a red line the $T_c \propto \lambda^{-0.43}$ power law inferred from those measurements.

additional, $T^{3=2}$ temperature dependence to $s(T)$ that should become progressively more important on underdoping, with the theory predicting a decline in the slope ds/dT similar to that seen in our experiment⁴³. However, our results show no sign of the $T^{3=2}$ power law in $s(T)$.

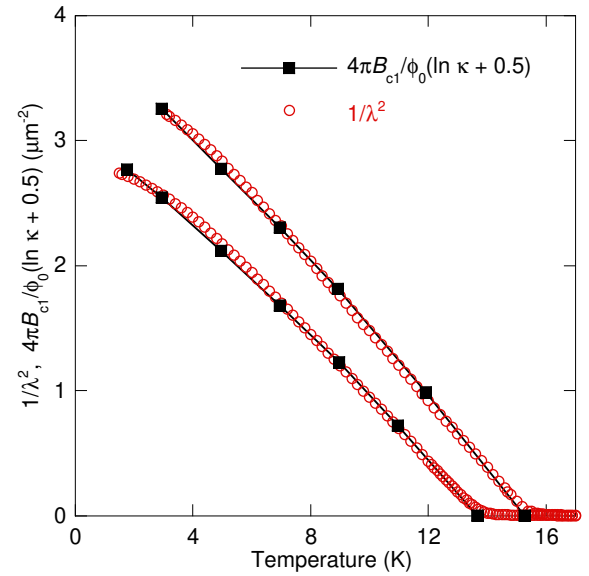


FIG. 6: Comparison of superfluid density and lower critical field. At the two dopings for which we have overlapping B_{c1} data³⁶ (squares) and $1/\lambda^2$ data (circles), a temperature independent $\kappa = 50$ is used to match B_{c1} and $1/\lambda^2$ via $1/\lambda^2 = 4\pi B_{c1}/\phi_0 (\ln \kappa + \frac{1}{2})$. For the $T_c = 13.7$ K doping we obtain $\kappa = 105$ and $\phi_0(T=0) = 51$ A. For the $T_c = 15.3$ K doping we obtain $\kappa = 90$ and $\phi_0 = 54$ A.

A recent approach to the behaviour of $s(T)$ invokes quantum criticality as the key to understanding properties close to where T_c is driven to zero^{18,44}. In the vicinity of a quantum critical point, scaling theories acquire an extra effective dimension due to the effects of quantum fluctuations¹⁷. As was argued above, $\text{YBa}_2\text{Cu}_3\text{O}_{6+x}$ behaves as a 3-dimensional superconductor and there is considerable evidence that it exhibits 3D XY critical fluctuations at higher doping⁴⁵. In particular, the phase stiffness near T_c gives $s(T) \propto \sqrt{T_c - T}$, with ν taking on the 3D XY value of $2=3$ ⁴⁶. If the transition from superconductor to non-superconductor illustrated in Fig 1 is a continuous phase transition rather than first-order, then the behaviour is governed by a quantum critical point at x_c with $(3+z)D$ -XY critical fluctuations, where $z \geq 1$ is the dynamical critical exponent. Since 4D is the upper critical dimension for the XY model, exponents near the transition are expected to revert to mean field behaviour, as is observed in Fig. 3 where $s(T) \propto \sqrt{T_c - T}$.

The approach to the quantum critical point has implications for the doping dependence of s . Figure 5a shows the correlation between T_c and $s_0 = 1/\lambda^2(T=0)$, obtained by both linear and quadratic extrapolation to $T = 0$. The data follow an approximately square-root power law. The new data are plotted on logarithmic axes in Fig. 5b alongside existing data for single crystal $\text{YBa}_2\text{Cu}_3\text{O}_{6+x}$. These include: very recent μSR data on single crystals⁴⁰; data from Gd^{3+} ESR, taking the ab-plane geometric mean³⁹; and B_{c1} data³⁶, converted to superfluid density assuming that $\kappa = 50$. The sublinear cor-

relation continues to optimal doping, although the data cannot be described by a single power law over the whole doping range. A recent study on thin film $\text{YBa}_2\text{Cu}_3\text{O}_{6+x}$ has found a qualitatively similar result, $T_c / \rho_{s0}^{0.43}$, which we include in Fig. 5b as the solid red line⁴¹. However, the superfluid density in the thin films is as much as 8 times lower than in single-crystal $\text{YBa}_2\text{Cu}_3\text{O}_{6+x}$ of the same T_c . This could be due to grain-boundary effects or increased levels of disorder, but the basic trend survives whatever extra disorder there is in the thin films. One of the motivations for carrying out measurements of ρ_s in the highly underdoped regime is that the scaling theory of the fluctuating d-wave superconductor^{17,18} makes clear predictions for the correlation between T_c and ρ_{s0} . Our experiment is uniquely positioned to test these predictions, as in underdoped $\text{YBa}_2\text{Cu}_3\text{O}_{6.333}$ we can tune through this doping range in a single sample, without changing cation disorder or introducing significant inhomogeneity. In two dimensions the scaling theory predicts T_c / ρ_{s0} , independent of universality class and dynamical critical exponent, along with the abrupt drop in $\rho_s(T)$ at T_c associated with a transition governed by vortex unbinding. While early experiments found evidence for an approximately linear correlation between T_c and ρ_{s0} ¹⁰, the latest data on $\text{YBa}_2\text{Cu}_3\text{O}_{6+x}$ do not support this, particularly at the lowest dopings. Instead, the observed behaviour is closer to $T_c / \rho_{s0}^{0.5}$, which is what scaling predicts in the vicinity of a (3+1)D XY quantum critical point^{29,47}.

To address the influence that fluctuations have on the slope $d\rho_s/dT$ Franz and Iyengar go beyond the scaling arguments to include the influence of nodal quasiparticles. They use an excitation spectrum characterized by a large energy gap due to strong superconducting pairing (corresponding to a large value of v in Eq. 1). Within this framework they calculate the renormalization of ρ_{s0} and the effective quasiparticle charge, and find behaviour in qualitative accord with our experimental observations, namely a phase stiffness that declines rapidly with T_c and a slope to the temperature dependence that also declines with T_c . A further clue to the large energy scale for the superconducting pairing can be found by comparing the superfluid density data to measurements of the first critical field B_{c1} made on similar $\text{YBa}_2\text{Cu}_3\text{O}_{6+x}$ samples³⁶. The dominant contribution to B_{c1} comes from the kinetic energy of the supercurrent flow around a vortex, which depends in detail on the short length-scale cut-off provided by the size of the vortex core ξ the superconducting coherence length ξ_0 . In BCS theory the first critical field is given by

$$B_{c1} = \frac{\phi_0}{4} \ln \left(\frac{\xi_0}{\xi} \right) + \frac{1}{2} \phi_0; \quad (2)$$

where $\phi_0 = \frac{h}{2e}$ and $\xi_0 = \hbar v / 2\Delta$ is the flux quantum. Therefore, a comparison of B_{c1} and ρ_s can be used to extract ξ . This process is shown in Fig. 6 for the two dopings at which we have overlapping B_{c1} and ρ_s data. We are able to achieve a good match between $\rho_s(T)$ and

$B_{c1}(T)$ using a temperature independent ξ . The zero-temperature coherence length obtained in the analysis, $\xi_0 = (\hbar v / 2\Delta) = \xi$, is very short, of the order of 50 Å. Furthermore, the doping dependence of the two measured quantities is different: $\rho_s(T) / T_c^2$ and $B_{c1} / T_c^{1.63}$, implying that ξ rises rapidly as the quantum critical point is approached. This suggests that although ξ is diverging (because Δ is falling to zero), ξ_0 continues to be very small due to the large pairing energy scale. A similar conclusion about ξ_0 has been drawn from high field measurements of the Nernst effect which probe the upper critical field B_{c2} ¹². Here we have shown that this short coherence length and its associated large pairing energy exist right down to the doping at which superconductivity gives way to magnetism in the cuprate phase diagram. This provides a key anchor point for understanding the cuprate phase diagram { a quantum critical point at which a strongly-paired superconductor becomes non-superconducting due to phase disorder. The next step will be to add fluctuating magnetism to this picture, as has been suggested by recent neutron scattering experiments that observed short-range, fluctuating spin correlations in $T_c = 18$ K $\text{YBa}_2\text{Cu}_3\text{O}_{6+x}$ ⁴⁸.

Methods

Sample preparation

Single crystals of $\text{YBa}_2\text{Cu}_3\text{O}_{6+x}$ were grown in barium zirconate crucibles and are extremely pure, with cation disorder at the 10^{-4} level⁴⁹. For this experiment a crystal 0.3 mm thick was cut and polished with Al_2O_3 abrasive into an ellipsoid 0.35 mm in diameter. The oxygen content of the ellipsoid was adjusted to $\text{O}_{6.333}$ by annealing at 914 C in flowing oxygen, followed by a homogenization anneal in a sealed quartz ampoule at 570 C and a quench to 0 C. At this point the sample was non-superconducting. After allowing chain oxygen order to develop at room temperature for three weeks, T_c was 3 K. The sample was then further annealed at room temperature for six weeks under hydrostatic pressure of 21 kbar, raising T_c to 17 K. The sample was cooled to 0 C before removing from the pressure cell, and then stored at -10 C to prevent the oxygen order from relaxing. All further manipulation of the ellipsoid was carried out in a refrigerated glove box at temperatures less than -5 C. Periods of controlled oxygen disordering at room temperature and ambient pressure were used to generate a sequence of dopings as T_c relaxed back to 3 K. Subsequent reannealing under hydrostatic pressure of 30 kbar, for a further six weeks, returned T_c to the starting value of 17 K.

Measurement of superfluid density

Measurements of the ab-plane surface impedance $Z_s = R_s + iX_s$ were carried out at 5.48 GHz by cavity perturbation, using a sapphire hot-nger to

position the sample at the H -eld antinode of the TE₀₁ mode of a rutile dielectric resonator⁵⁰. The c-axis of the ellipsoid was oriented along the microwave H -eld, with nal alignment carried out using magnetic torque in a 7 T -eld. The surface impedance of the sample has been obtained from the measured cavity response using the cavity perturbation formula $f_B(T) - 2if_0(T) = (R_s + iX_s)$, where $f_B(T)$ is the change in bandwidth of the TE₀₁ mode upon inserting the sample into the cavity, and $f_0(T)$ is the shift in resonant frequency upon warming the sample

from base temperature to T. α is a scale factor that applies to the data set as a whole, and is empirically determined using Pb(Sn) replica samples to an accuracy of 2.5%. The absolute surface reactance is set by matching R_s and X_s in the normal state, where we expect the imaginary part of the microwave conductivity to be very small. The complex microwave conductivity $\sigma_s = \sigma_1 - i\sigma_2$ is obtained using the local-limit expression $\sigma_s = i!_0 = Z_s^2$, with the superfluid density given by $\sigma_2 = 1 = ^2(T) = !_0^2$.

- ¹ Orenstein, J. & Millis, A. J. Advances in the physics of high-temperature superconductivity. *Science* 288, 468(474 (2000)).
- ² Warren, W. W. et al. Cu spin dynamics and superconducting precursor effects in planes above T_c in YBa₂Cu₃O_{6.70}. *Phys. Rev. Lett.* 62, 1193(1196 (1989)).
- ³ Orenstein, J. et al. Frequency and temperature dependent conductivity in YBa₂Cu₃O_{6+x} crystals. *Phys. Rev. B* 42, 6342(6362 (1990)).
- ⁴ Homes, C. C., Timusk, T., Liang, R., Bonn, D. A. & Hardy, W. N. Optical conductivity of c axis oriented YBa₂Cu₃O_{6.70}: evidence for a pseudogap. *Phys. Rev. Lett.* 71, 1645(1648 (1993)).
- ⁵ Emery, V. J. & Kivelson, S. A. Importance of phase fluctuations in superconductors with small superfluid density. *Nature* 374, 434(437 (1995)).
- ⁶ Franz, M. & Tesanovic, Z. Algebraic fermi liquid from phase fluctuations: "topological" fermions, vortex "berryons," and QED₃ theory of cuprate superconductors. *Phys. Rev. Lett.* 87, 257003 (2001).
- ⁷ Franz, M., Tesanovic, Z. & Vafek, O. QED₃ theory of pairing pseudogap in cuprates: From d-wave superconductor to antiferromagnet via an algebraic fermi liquid. *Phys. Rev. B* 66, 054535 (2002).
- ⁸ Herbut, I. F. Antiferromagnetism from phase disordering of a d-wave superconductor. *Phys. Rev. Lett.* 88, 047006 (2002).
- ⁹ Herbut, I. F. QED₃ theory of underdoped high-temperature superconductors. *Phys. Rev. B* 66, 094504 (2002).
- ¹⁰ Uemura, Y. J. et al. Universal correlations between T_c and n_s/m (carrier density over effective mass) in high-T_c cuprate superconductors. *Phys. Rev. Lett.* 62, 2317(2320 (1989)).
- ¹¹ Corson, J., Malozzi, R., Orenstein, J., Eckstein, J. N. & Bozovic, I. Vanishing of phase coherence in underdoped Bi₂Sr₂CaCu₂O_{8+x}. *Nature* 398, 221(223 (1999)).
- ¹² Wang, Y. et al. Dependence of upper critical field and pairing strength on doping in cuprates. *Science* 299, 86(89 (2002)).
- ¹³ Anderson, P. W. The resonating valence bond state in La₂CuO₄. *Science* 235, 1196(1198 (1987)).
- ¹⁴ Io, L. B. & Larkin, A. I. Gapless fermions and gauge fields in dielectrics. *Phys. Rev. B* 39, 8988(8999 (1989)).
- ¹⁵ Lee, P. A. & Wen, X. G. Unusual superconducting state of underdoped cuprates. *Phys. Rev. Lett.* 78, 4111(4114 (1997)).
- ¹⁶ Wen, X. G. & Lee, P. A. Theory of quasiparticles in the underdoped high-T_c superconducting state. *Phys. Rev. Lett.* 80, 2193(2196 (1998)).
- ¹⁷ Sachdev, S. *Quantum Phase Transitions* (Cambridge University Press, 2001).
- ¹⁸ Kopp, A. & Chakravarty, S. Criticality in correlated quantum matter. *Nat. Phys.* 1, 53(56 (2005)).
- ¹⁹ Hosseini, A. et al. Survival of the d-wave superconducting state near the edge of antiferromagnetism in the cuprate phase diagram. *Phys. Rev. Lett.* 93, 107003 (2004).
- ²⁰ Liang, R. et al. Preparation and characterization of homogeneous YBCO single crystals with doping level near the SC/AFM boundary. *Physica C* 383, 1(7 (2002)).
- ²¹ Liang, R., Bonn, D. A. & Hardy, W. N. Evaluation of CuO₂ plane hole doping in YBa₂Cu₃O_{6+x} single crystals. Preprint at <http://xxx.lanl.gov/pdf/cond-mat/0510674> (October 2005).
- ²² Zaanen, J., Paxton, A. T., Jepsen, O. & Andersen, O. K. Chain-fragment doping and the phase diagram of YBa₂Cu₃O_{7-x}. *Phys. Rev. Lett.* 60, 2685(2688 (1988)).
- ²³ Veal, B. W. et al. Observation of temperature-dependent site disorder in YBa₂Cu₃O₇ below 150 C. *Phys. Rev. B* 42, 6305(6316 (1990)).
- ²⁴ Fisher, D. S., Fisher, M. P. A. & Huse, D. A. Thermal fluctuations, quenched disorder, phase transitions, and transport in type-II superconductors. *Phys. Rev. B* 43, 130(159 (1991)).
- ²⁵ Bonn, D. A. et al. Comparison of the influence of Ni and Zn impurities on the electromagnetic properties of YBa₂Cu₃O_{6.95}. *Phys. Rev. B* 50, 4051(4063 (1994)).
- ²⁶ Hirschfeld, P. J. & Goldenfeld, N. Effect of strong scattering on the low-temperature penetration depth of a d-wave superconductor. *Phys. Rev. B* 48, R4219(4222 (1993)).
- ²⁷ Hirschfeld, P. J., Putikka, W. O. & Scalapino, D. J. d-wave model for the microwave response of high-T_c superconductors. *Phys. Rev. B* 50, 10250(10264 (1994)).
- ²⁸ Io, L. B. & Millis, A. J. d-wave superconductivity in doped Mott insulators. *J. Phys. Chem. Solids* 63, 2259(2268 (2002)).
- ²⁹ Herbut, I. F. & Case, M. J. Finite temperature superfluid density in very underdoped cuprates. *Phys. Rev. B* 70, 094516 (2004).
- ³⁰ Zuev, Y. et al. The role of thermal phase fluctuations in underdoped YBCO films. Preprint at <http://xxx.lanl.gov/pdf/cond-mat/0407113> (July 2004).
- ³¹ Millis, A. J. et al. Anomalous charge dynamics in the superconducting state of underdoped cuprates. *J. Phys.*

- Chem. Solids 59, 1742{1744 (1998).
- ³² Herbut, I. F. Effective theory of high-temperature superconductors. Phys. Rev. Lett. 94, 237001 (2005).
- ³³ Case, M. & Herbut, I. F. Screening in anisotropic superfluids and the superfluid density in underdoped cuprates. Phys. Rev. B 72, 104503 (2005).
- ³⁴ Durst, A. C. & Lee, P. A. Impurity-induced quasiparticle transport and universal limit violation in d-wave superconductors. Phys. Rev. B 62, 1270{1290 (2000).
- ³⁵ Zhou, X. J. et al. Universal nodal Fermi velocity. Nature 423, 398{398 (2003).
- ³⁶ Liang, R., Bonn, D. A., Hardy, W. N. & Broun, D. Lower critical field and superfluid density of highly underdoped $\text{YBa}_2\text{Cu}_3\text{O}_{6+x}$ single crystals. Phys. Rev. Lett. 94, 117001 (2005).
- ³⁷ Lang, K. M. et al. Imaging the granular structure of high- T_c superconductivity in underdoped $\text{Bi}_2\text{Sr}_2\text{CaCu}_2\text{O}_{8+x}$. Nature 415, 412{416 (2002).
- ³⁸ Sheehy, D. E., Davis, T. P. & Franz, M. Unified theory of the ab-plane and c-axis penetration depths of underdoped cuprates. Phys. Rev. B 70, 054510 (2004).
- ³⁹ Pereg-Bamea, T. et al. Absolute values of the London penetration depth in $\text{YBa}_2\text{Cu}_3\text{O}_{6+x}$ measured by zero-field ESR spectroscopy on Gd-doped single crystals. Phys. Rev. B 69, 184513 (2004).
- ⁴⁰ Sonier, J. E. et al. Insulating antiferromagnetic vortex core state in under-doped $\text{YBa}_2\text{Cu}_3\text{O}_y$. Preprint at <http://xxx.lanl.gov/pdf/cond-mat/0508079> (August 2005).
- ⁴¹ Zuev, Y., Kin, M. S. & Lemberger, T. R. Correlation between superfluid density and T_c of underdoped $\text{YBa}_2\text{Cu}_3\text{O}_{6+x}$ near the superconductor{insulator transition. Phys. Rev. Lett. 95, 137002 (2005).
- ⁴² Chen, Q., Stavic, J. & Levin, K. Applying BCS{BEC crossover theory to high temperature superconductors and ultracold atomic fermi gases. Preprint at <http://xxx.lanl.gov/pdf/cond-mat/0508603> (August 2005).
- ⁴³ Chen, Q. J., Kosztin, I., Jankó, B. & Levin, K. Pairing fluctuation theory of superconducting properties in underdoped to overdoped cuprates. Phys. Rev. Lett. 81, 4708{4711 (1998).
- ⁴⁴ Franz, M. & Iyengar, A. P. Superfluid density of strongly underdoped cuprate superconductors from a four-dimensional XY model. Phys. Rev. Lett. 96, 047007 (2006).
- ⁴⁵ Mengast, C. et al. Phase fluctuations and the pseudogap in $\text{YBa}_2\text{Cu}_3\text{O}_{6+x}$. Phys. Rev. Lett. 86, 1606{1609 (2001).
- ⁴⁶ Kamal, S. et al. Penetration depth measurements of 3D XY critical behaviour in $\text{YBa}_2\text{Cu}_3\text{O}_{6.95}$ crystals. Phys. Rev. Lett. 73, 1845{1848 (1994).
- ⁴⁷ Millis, A. Effect of a non-zero temperature on quantum critical points in itinerant fermion systems. Phys. Rev. B 48, 7183{7196 (1993).
- ⁴⁸ Stock, C. et al. Central mode and spin confinement near the boundary of the superconducting phase in $\text{YBa}_2\text{Cu}_3\text{O}_{6.353}$ ($T_c = 18$ K). Preprint at <http://xxx.lanl.gov/pdf/cond-mat/0505083> (May 2005).
- ⁴⁹ Liang, R., Bonn, D. A. & Hardy, W. N. Growth of high quality YBCO single crystals using BaZrO_3 crucibles. Physica C 304, 105{111 (1998).
- ⁵⁰ Huttema, W. A. et al. Apparatus for high resolution microwave spectroscopy in strong magnetic fields. Rev. Sci. Instrum. 77, 023901 (2006).

Competing financial interests

The authors declare that they have no competing financial interests.

Acknowledgements

We acknowledge useful discussions with M. J. Case, S. Chakravarty, J. S. Dodge, M. Franz, I. F. Herbut, S. A. Kivelson and J. E. Sonier. This work was funded by the National Science and Engineering Research Council of Canada and the Canadian Institute for Advanced Research.

Correspondence and requests for materials should be directed to D. M. B. or D. A. B.